Hydrology and Earth System Sciences

Supporting Information for

Proposing Sources for Discrete Groundwater Discharges to Patterned Pools in Three Regional Raised Northern Peat Bogs

Henry E. Moore[1], Xavier Comas[2], Martin A. Briggs[3], Andrew S. Reeve[4], Khondaker Md. Nur Alam[1], Lee Slater[1,5]

[1]Rutgers University Newark, Department of Earth, and Environmental Sciences, 101 Warren St. Smith Hall – Room 135 Newark, NJ 07102, United States of America
[2]Florida Atlantic University, Department of Geosciences, 777 Glades Road, Boca Raton, FL 33431, United States of America
[3]U.S. Geological Survey, Observing Systems Division, Hydrologic Remote Sensing Branch, 11 Sherman Place, Unit 5015, Storrs, CT 06269, United States of America
[4]University of Maine, School of Earth and Climate Sciences, 5790 Bryand Global Sciences Center, Orono, ME 04469-5790, United States of America
[5]Pacific Northwest National Laboratory, 902 Battelle Blvd, Richland, WA 99354 United States of America

Correspondence to: Henry E. Moore (hem62@rutgers.edu)

Disclaimer: Any use of trade, firm, or product names is for descriptive purposes only and does not imply endorsement by the U.S. Government

Contents of this file

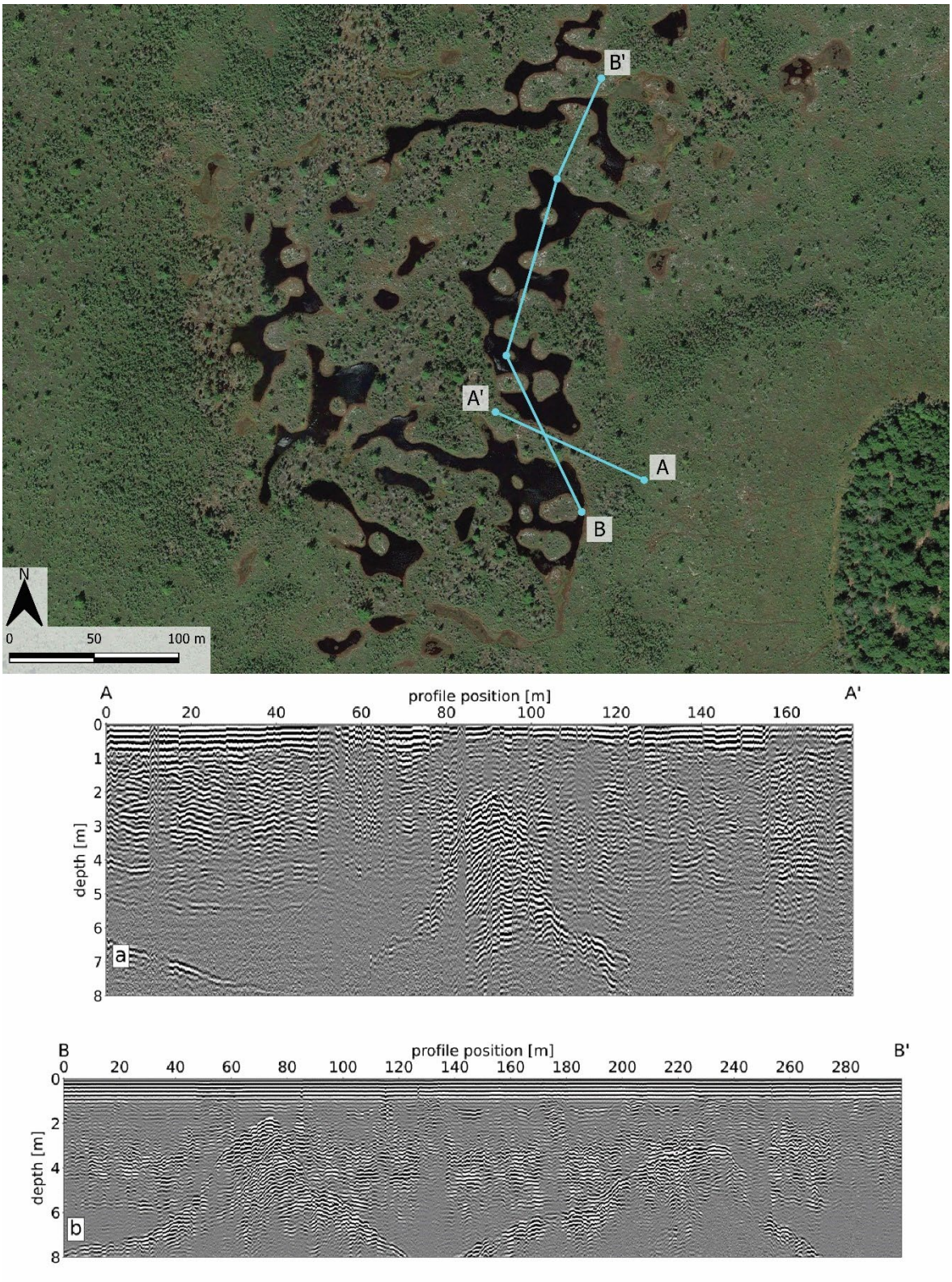

Figure S1: Select supplementary GPR transects (velocity = 0.0360 m/ns) from Comas et al. (2011) displaying glacial esker ridges correlating with the eastern edge of the patterned pools of Caribou Bog. Basemap data: © Microsoft (2024).

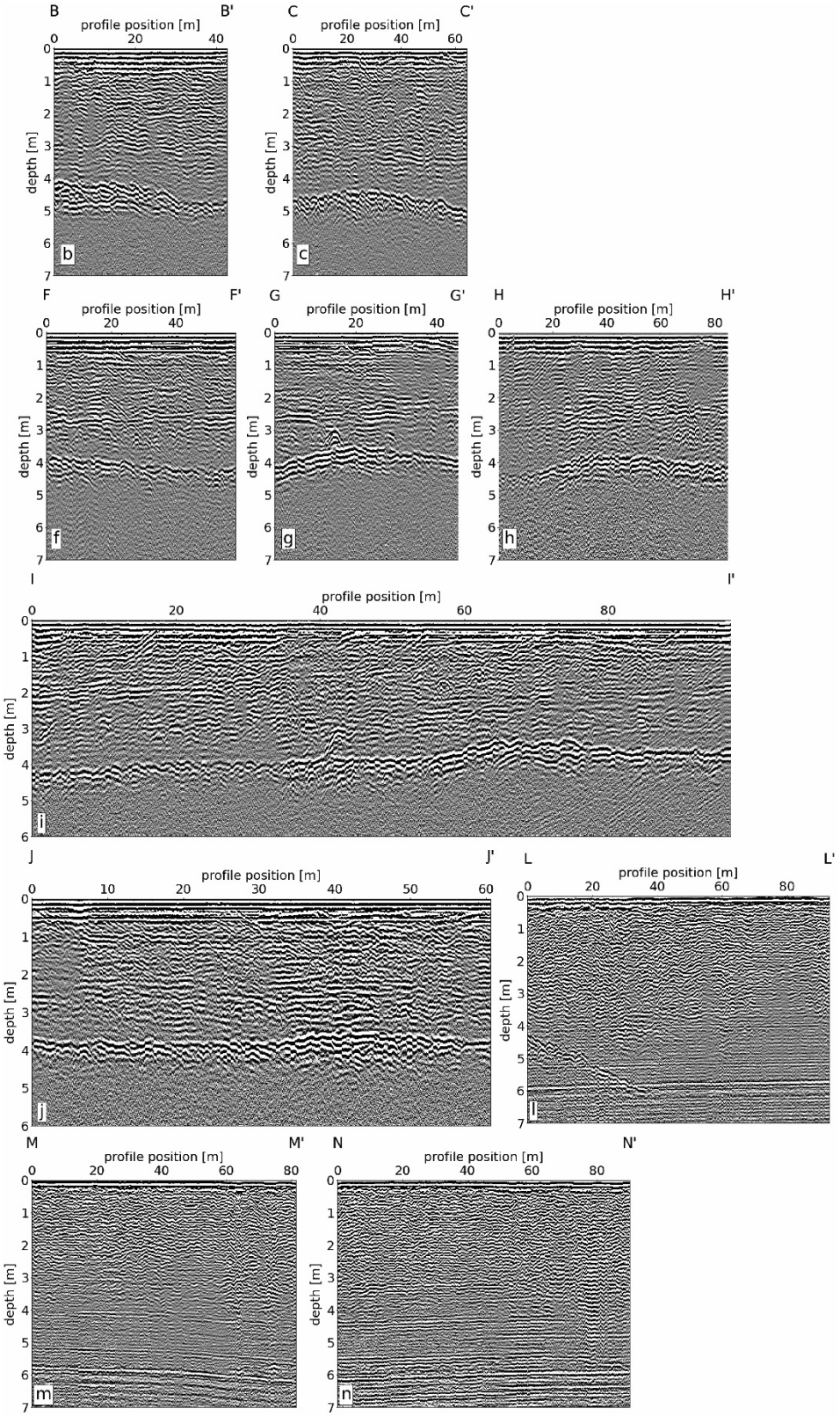

Figure S2: Additional GPR transects (velocity = 0.0360 m/ns) collected around the patterned pools of Thousand Acre (Crystal) Bog.

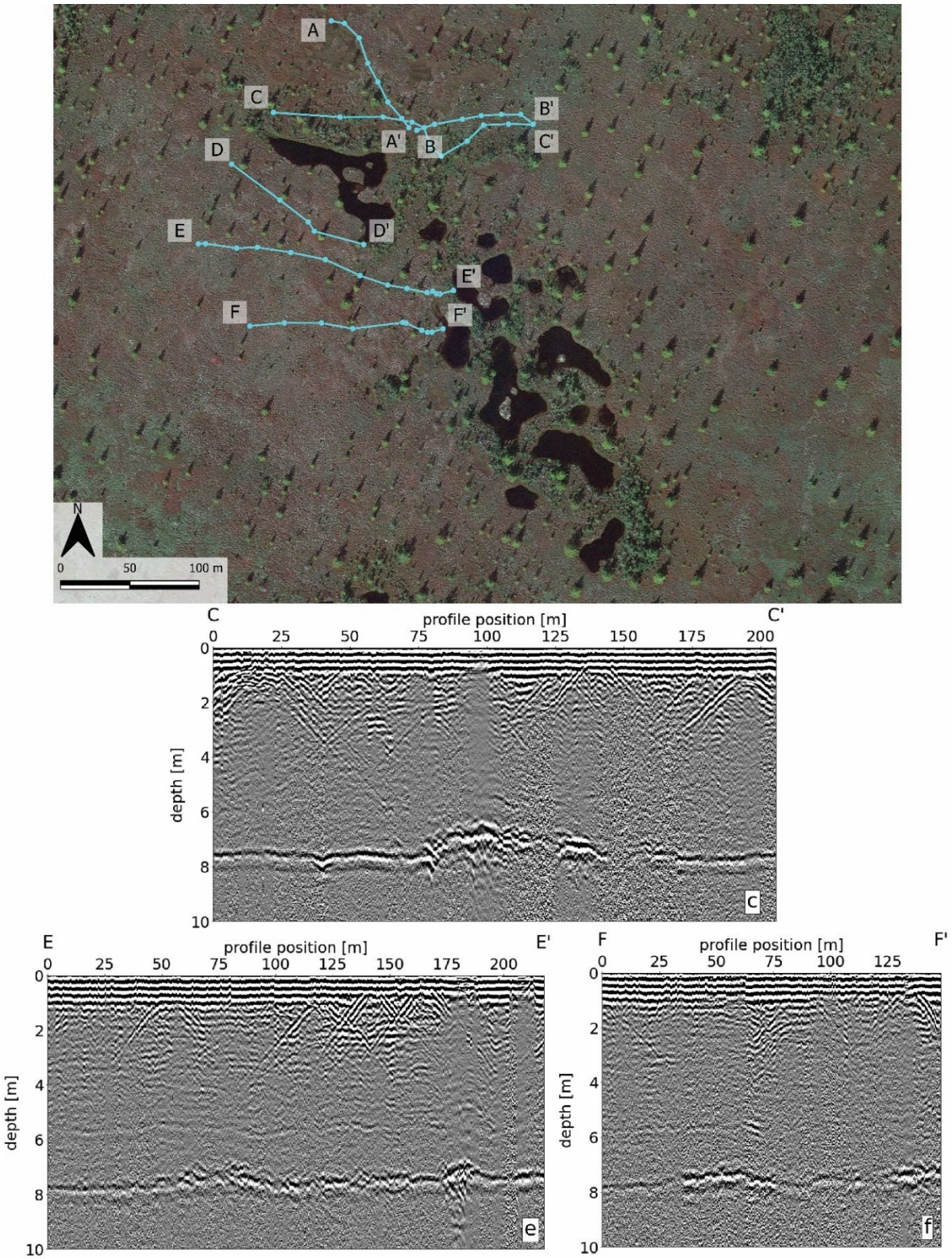

Figure S3: GPR transects (velocity = 0.0360 m/ns) collected around the patterned pools of Meddybemps Heath, indicating the locations of mineral sediment discontinuities relative to the surface of the peatland. Basemap data: © Microsoft (2024).

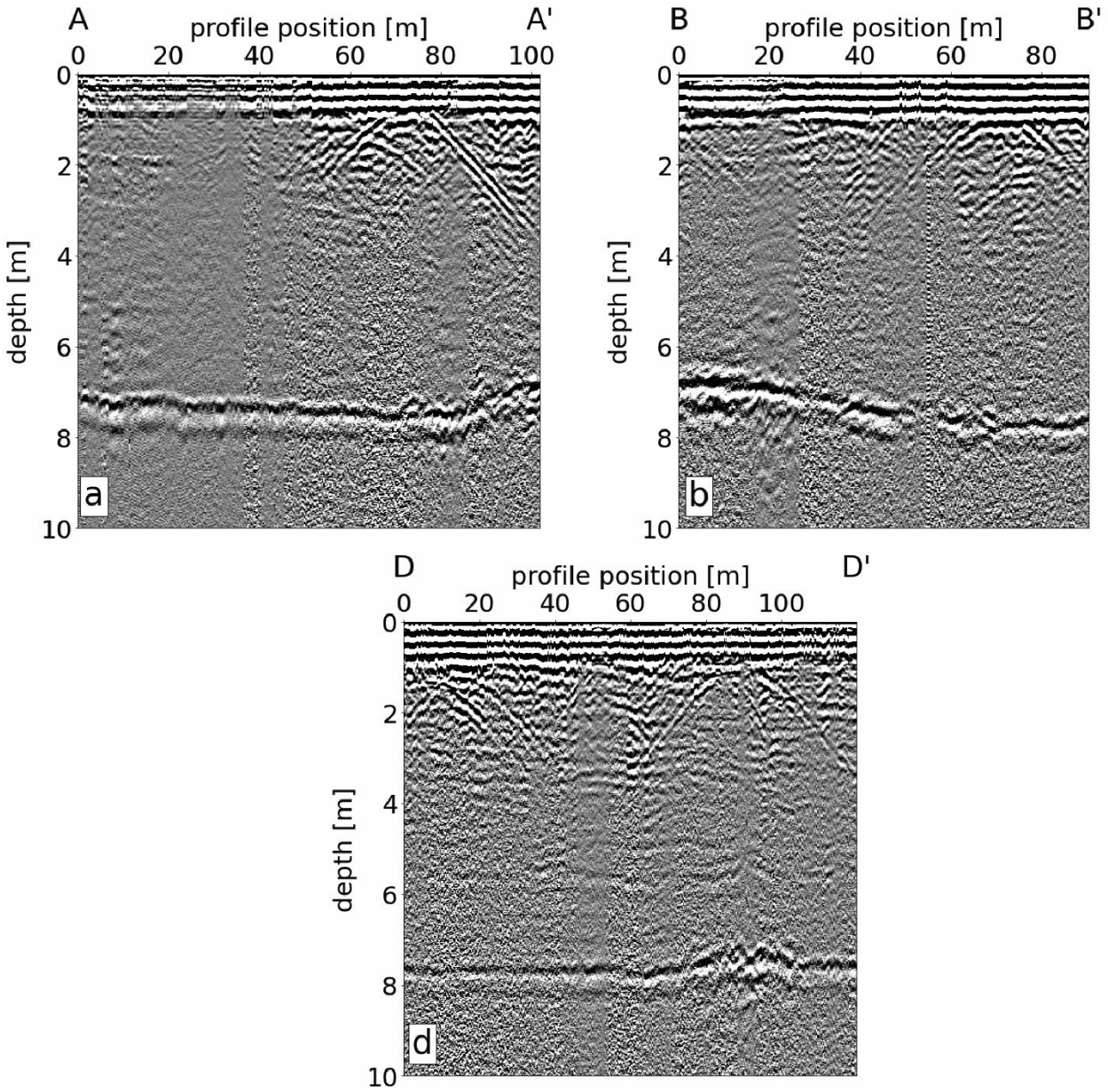

Figure S4: Additional GPR transects (velocity = 0.0360 m/ns) collected around the patterned pool system in Meddybemps Heath.

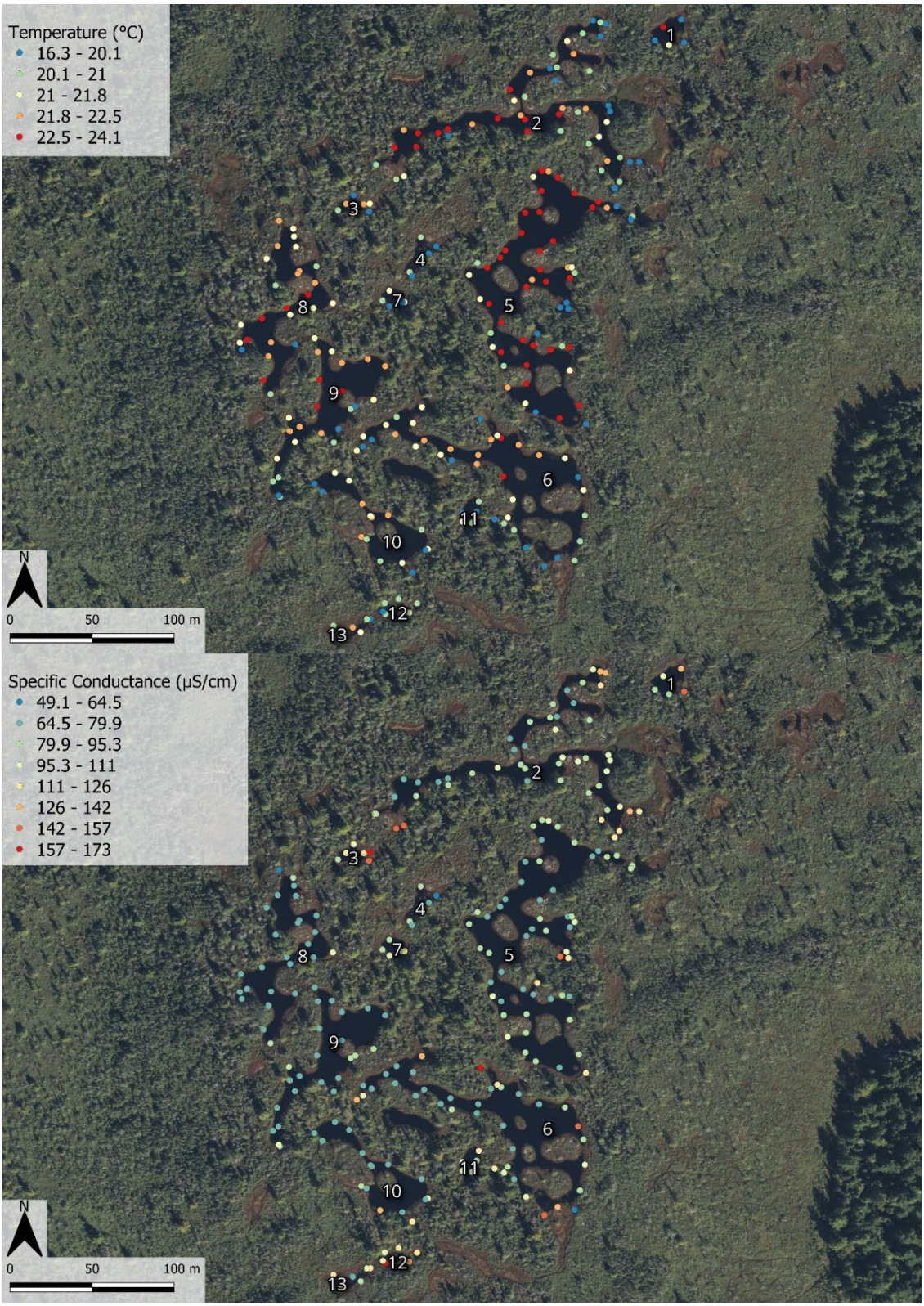

Figure S5: Temperature (ºC) and Specific Conductance (µS/cm) collected around the patterned peatland pools (n=13) of Caribou Bog on August 23rd, 2022, and August 24th, 2022. Basemap data: © Microsoft (2024).

Table S1. Sample size, coefficient of determination, slope, and interpreted dominant water source for 13 patterned peatland pools analyzed in Caribou Bog.

Pool Number	Sample Size (n)	Coefficient of Determination (R^2)	Slope (m)	p-value (p)
1	5	0.326	-9.04	0.315
2	49	0.191	-4.99	0.00172
3	7	0.0217	3.82	0.753
4	6	0.960	9.69	0.000608
5	55	0.466	-6.58	9.30E-9
6	37	0.197	-9.00	0.00591
7	5	0.00530	1.17	0.908
8	26	0.112	-3.21	0.0942
9	24	0.455	-6.08	0.000302
10	17	0.115	-6.52	0.184
11	4	0.000400	0.914	0.979
12	6	0.196	22.0	0.38
13	6	0.623	-16.4	0.062

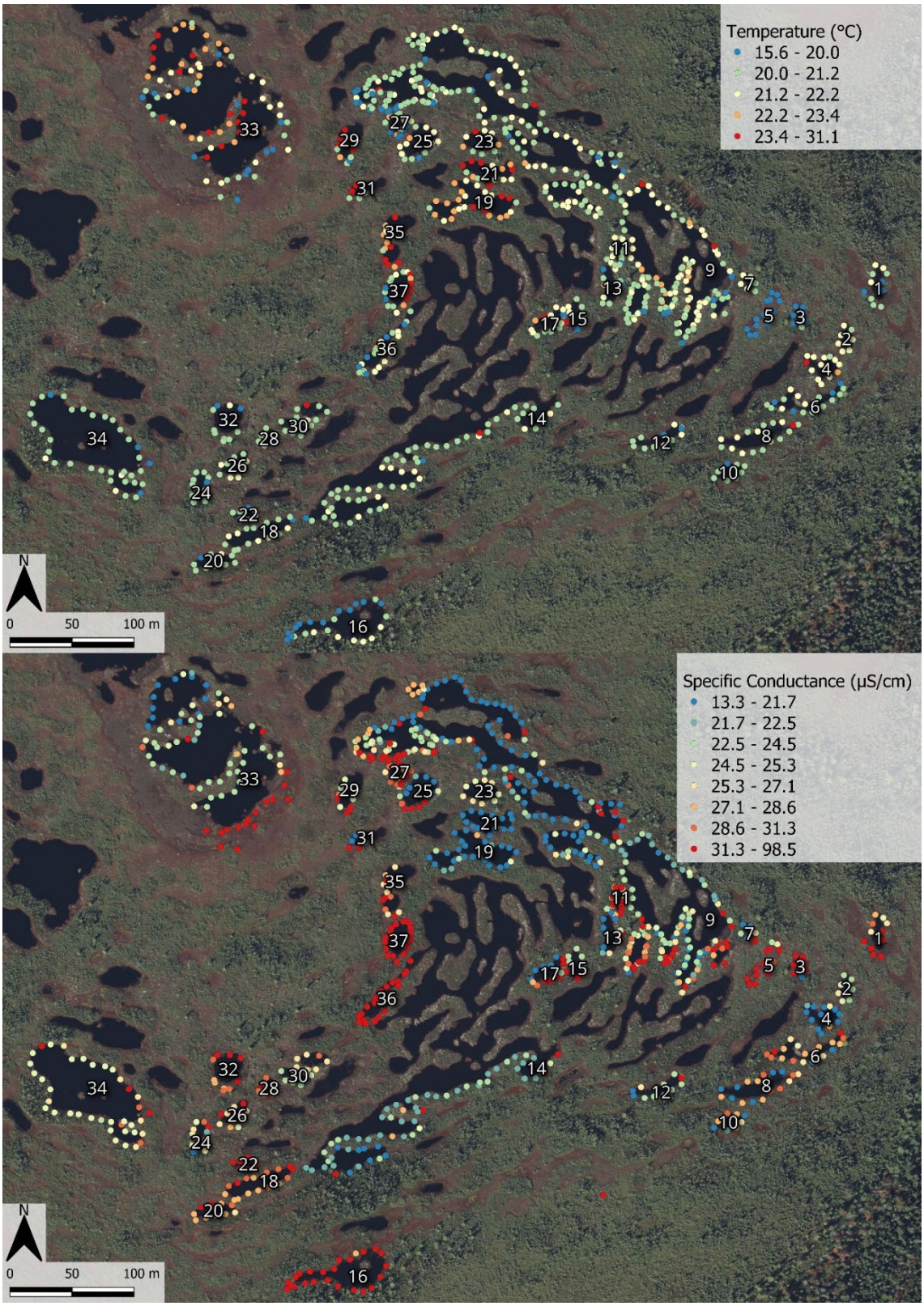

Figure S6: Temperature (°C) and Specific Conductance (µS/cm) collected around the patterned peatland pools (n=37) of Thousand Acre (Crystal) Bog on August 8th, 2023, August 10th, 2023, and August 15th, 2023. Basemap data: © Microsoft (2024).

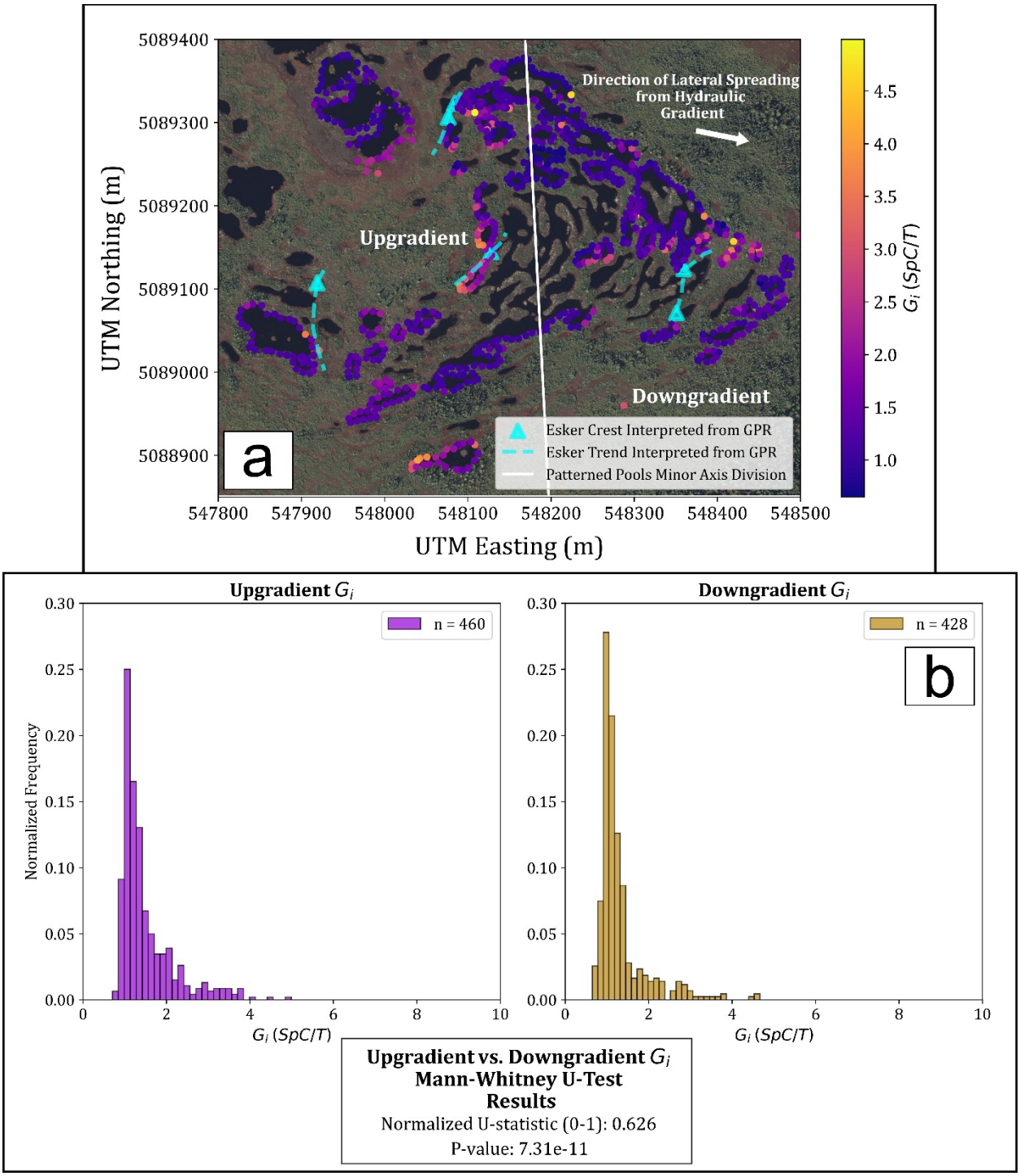

Figure S7: Groundwater indicator (G_i) values (n = 888), in a) given as ratios of specific conductance (µS/cm) to temperature (ºC) collected at 0.25-meters depth along the perimeter of patterned pools (n = 37) of Thousand Acre (Crystal) Bog with interpreted trends of underlying glacial esker deposits inferred from GPR data, and the inferred direction of lateral spreading for the pool system. Histograms in b) show the normalized frequency of G_i values of the upgradient and downgradient sections, split by the major axis of the patterned pool system. In b), a Mann-Whitney U-Test shows a significant p-value for the difference between

the two populations, and a normalized U-statistic demonstrates the upgradient side of the pools consists of statistically larger G_i values than the downgradient side of the pools. Basemap data: © Microsoft (2024).

Table S2. Sample size, coefficient of determination, slope, and interpreted dominant water source for 37 patterned peatland pools analyzed in Thousand Acre (Crystal) Bog.

Pool Number	Sample Size (n)	Coefficient of Determination (R^2)	Slope (m)	p-value (p)
1	11	0.560	-12.8	0.00804
2	7	0.280	0.996	0.222
3	7	0.709	-29.9	0.0175
4	13	0.489	-5.28	0.00778
5	11	0.144	20.8	0.250
6	19	0.430	-4.13	0.00231
7	7	0.408	-7.53	0.122
8	17	0.00740	0.313	0.742
9	294	0.194	-4.18	2.66E-15
10	8	0.335	-3.48	0.133
11	16	0.585	-13.8	0.000560
12	13	0.286	-4.62	0.0598
13	11	0.560	-2.31	0.00805
14	60	0.401	-3.67	5.55E-8
15	8	0.162	-3.97	0.323
16	23	0.507	-6.60	0.000137
17	12	0.554	-9.06	0.00553
18	16	0.460	-5.51	0.00389
19	26	0.0560	-0.400	0.244
20	10	0.299	-3.15	0.102
21	14	0.0698	-0.0510	0.362
22	7	0.00780	0.353	0.851
23	9	0.0260	-0.0510	0.679
24	10	0.0985	2.31	0.377
25	13	0.584	-12.5	0.00235
26	9	0.0116	-1.44	0.783
27	15	0.195	-4.14	0.0999
28	6	0.0146	0.371	0.820
29	9	0.588	-6.21	0.0160
30	14	0.0219	0.193	0.614
31	5	0.515	-4.33	0.172
32	10	0.0206	-1.60	0.692
33	78	0.197	-2.16	4.71E-5
34	38	0.0140	-1.19	0.479
35	12	0.418	-6.08	0.0231
36	23	0.0747	-1.86	0.207
37	18	0.559	-5.28	0.000361

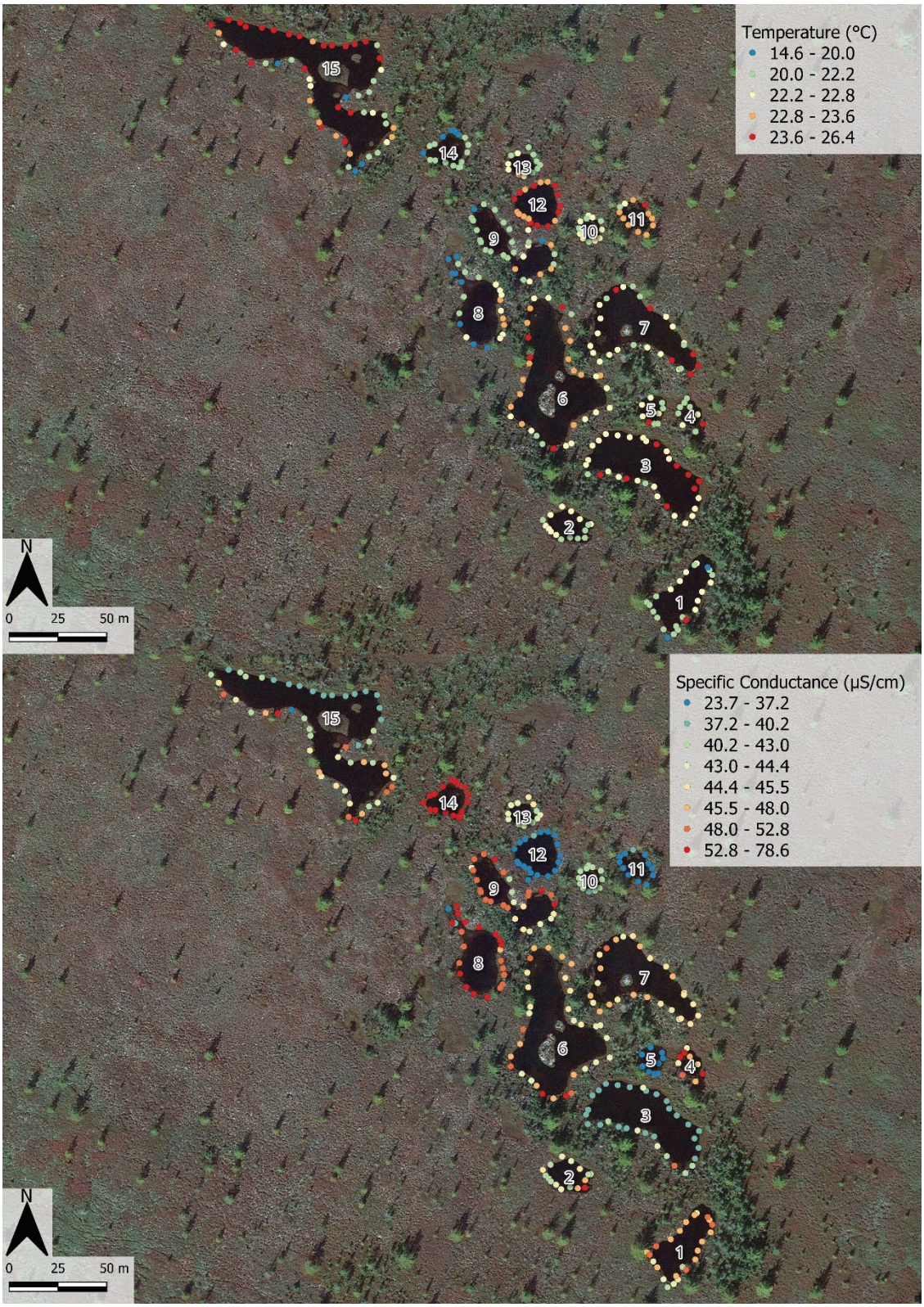

Figure S8: Temperature (ºC) and specific conductance (µS/cm) collected around the patterned pools (n=15) of Meddybemps Heath on August 7th, 2023, and August 17th, 2023. Basemap data: © Microsoft (2024).

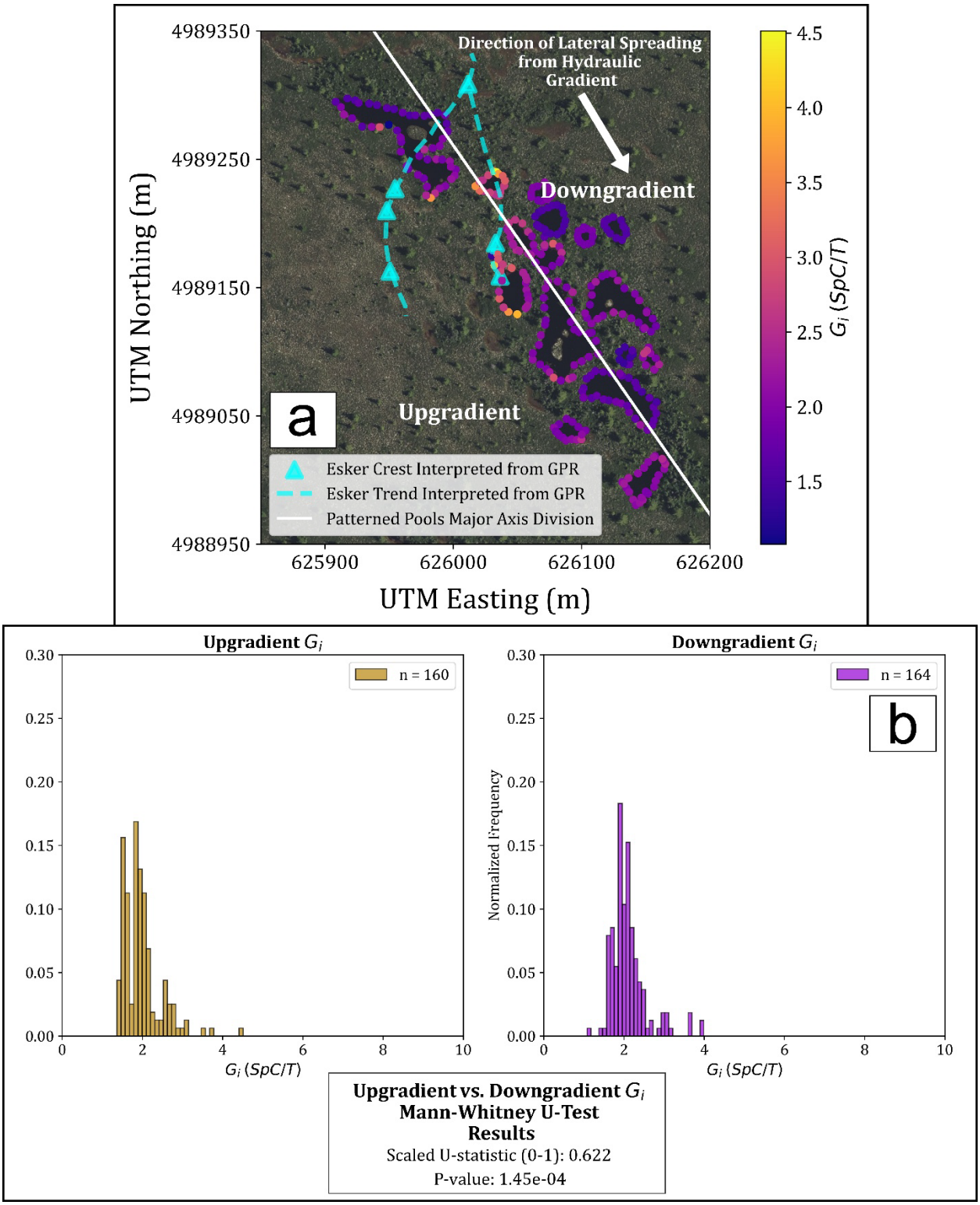

Figure S9: Groundwater indicator (G_i) values (n = 324), in a) given as ratios of specific conductance (µS/cm) to temperature (ºC) collected at 0.25-meters depth along the perimeter of patterned pools (n = 15) of Meddybemps Heath with interpreted trends of underlying glacial esker deposits inferred from GPR data, and the inferred direction of lateral spreading for the pool system. Histograms in b) show the normalized

frequency of G_i values of the upgradient and downgradient sections, split by the major axis of the patterned pool system. In b), a Mann-Whitney U-Test shows a significant p-value for the difference between the two populations, and a scaled U-statistic demonstrates that the upgradient side of the pools has statistically larger G_i values than the downgradient side of the pools. Basemap data: © Microsoft (2024).

Table S3. Sample size, coefficient of determination, slope, and interpreted dominant water source for 15 patterned peatland pools analyzed in Meddybemps Heath.

Pool Number	Sample Size (n)	Coefficient of Determination (R^2)	Slope (m)	p-value (p)
1	24	0.121	0.651	0.0959
2	16	0.143	-1.22	0.149
3	31	0.00140	-0.0950	0.839
4	10	0.0526	1.14	0.553
5	9	0.205	0.205	0.221
6	32	0.217	-1.89	0.00723
7	25	0.213	-0.642	0.0203
8	24	0.0896	0.313	0.155
9	28	0.147	-1.47	0.0442
10	12	0.501	1.13	0.0100
11	12	0.00340	0.0780	0.857
12	19	0.122	-0.419	0.142
13	12	0.00150	0.0350	0.905
14	18	0.176	-0.974	0.0833
15	51	0.244	-1.40	0.000233

Table S4. Tabulated local precipitation values from local NOAA weather stations prior to the five UAS TIR mapping surveys conducted in Caribou Bog, Meddybemps Heath, and Thousand Acre (Crystal) Bog Modified from NOAA (2023).

Patterned Pools Surveyed	Date of UAS TIR Survey	Precipitation Three Days Prior (mm)	Precipitation 24 Hours Before (mm)	NOAA Weather Station Location
Caribou Bog	June 9th, 2023	21.6	4.06	Orono, Maine, USA
Meddybemps Heath	June 15th, 2023	1.27	0.510	Cooper, Maine, USA
Meddybemps Heath	August 9th, 2023	29.0	29.0	Cooper, Maine, USA
Thousand Acre (Crystal) Bog	August 10th, 2023	22.9	19.8	Houlton, Maine, USA
Meddybemps Heath	November 3rd, 2023	NR	NR	Cooper, Maine, USA

Text S1. UAS TIR Mapping Survey Details

Imagery positioning was enhanced beyond the standard integrated GPS in the DJI M2EA (SZ DJI Technology Co., Ltd., Shenzhen, China) by using an external real time kinematic (RTK) module attached to the top of the aircraft. RGB and TIR imagery were collected by defining a flight pattern with the DJI Pilot app (SZ DJI Technology Co., Ltd., Shenzhen, China), integrated in the handheld controller of the UAS. Flights occurred at an altitude of 60 meters and at a speed of 1.83 m/s. The Side Overlap Ratio of the surveys was set to between 75% and 80% while the Front

Overlap Ratio was set to 80% to ensure adequate coverage of surveyed pools. External microSD cards were used to store RGB and TIR imagery captured during the missions. ThermoConverter software (Aetha, 2023) was used to transform all raw TIR imagery from the FLIR radiometric (rJPEG) formats into 16-bit TIFF files. Agisoft Metashape Professional software was then used to combine individual RGB and TIR imagery into cohesive orthomosaic maps of the pools. The parameters used in Agisoft Metashape Professional (Agisoft LLC, St. Petersburg, Russia), for each RGB and TIR orthomosaic, are outlined in the supplemental materials. The parameters used in Agisoft Metashape Professional, for each RGB and TIR orthomosaic, are outlined in the Tables S5 through S9. Temperature ranges of the TIR orthomosaic maps were calibrated using a linear regression technique developed by Harvey et al. (2019). A strong linear relationship between hand-measured temperature and TIR temperature values was established (coefficients of determination (R^2) varied between 0.992 and 0.997). The linear regression equation generated for each survey was used to calibrate the temperature ranges of TIR orthomosaic maps.

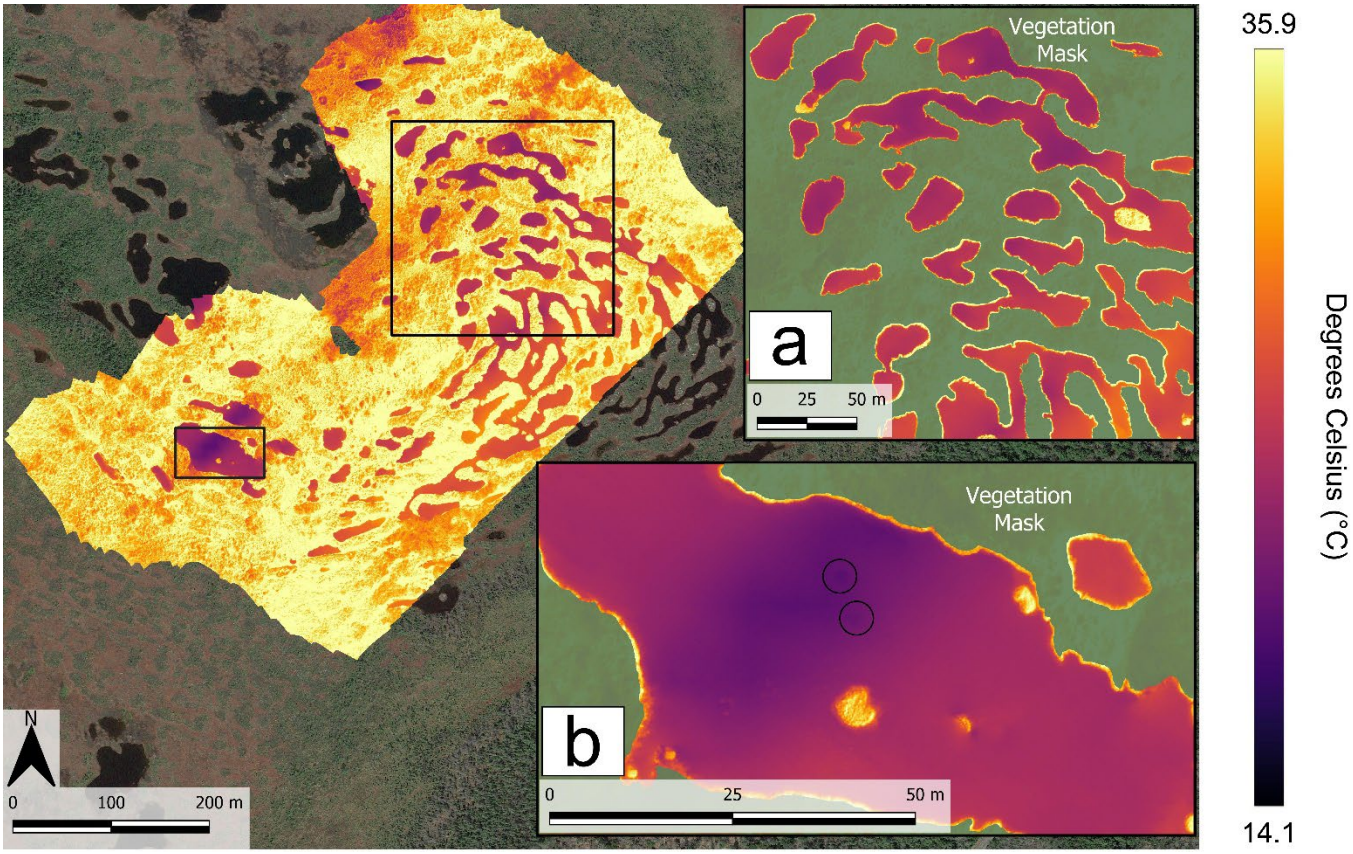

Figure S10: Unmanned Aerial System (UAS) Thermal Infrared (TIR) orthomosaic map, calibrated against the thermal emissivity of water, of the patterned pools in Thousand Acre (Crystal) Bog highlighting a thermal gradient originating from both the (a) north and (b) southwest sections of the pools, with warmer temperatures observed moving eastwards. Resolution of the TIR orthomosaic map is 8.16 cm/pixel and TIR imagery was collected on August 10th, 2023. Basemap data: © Microsoft (2024).

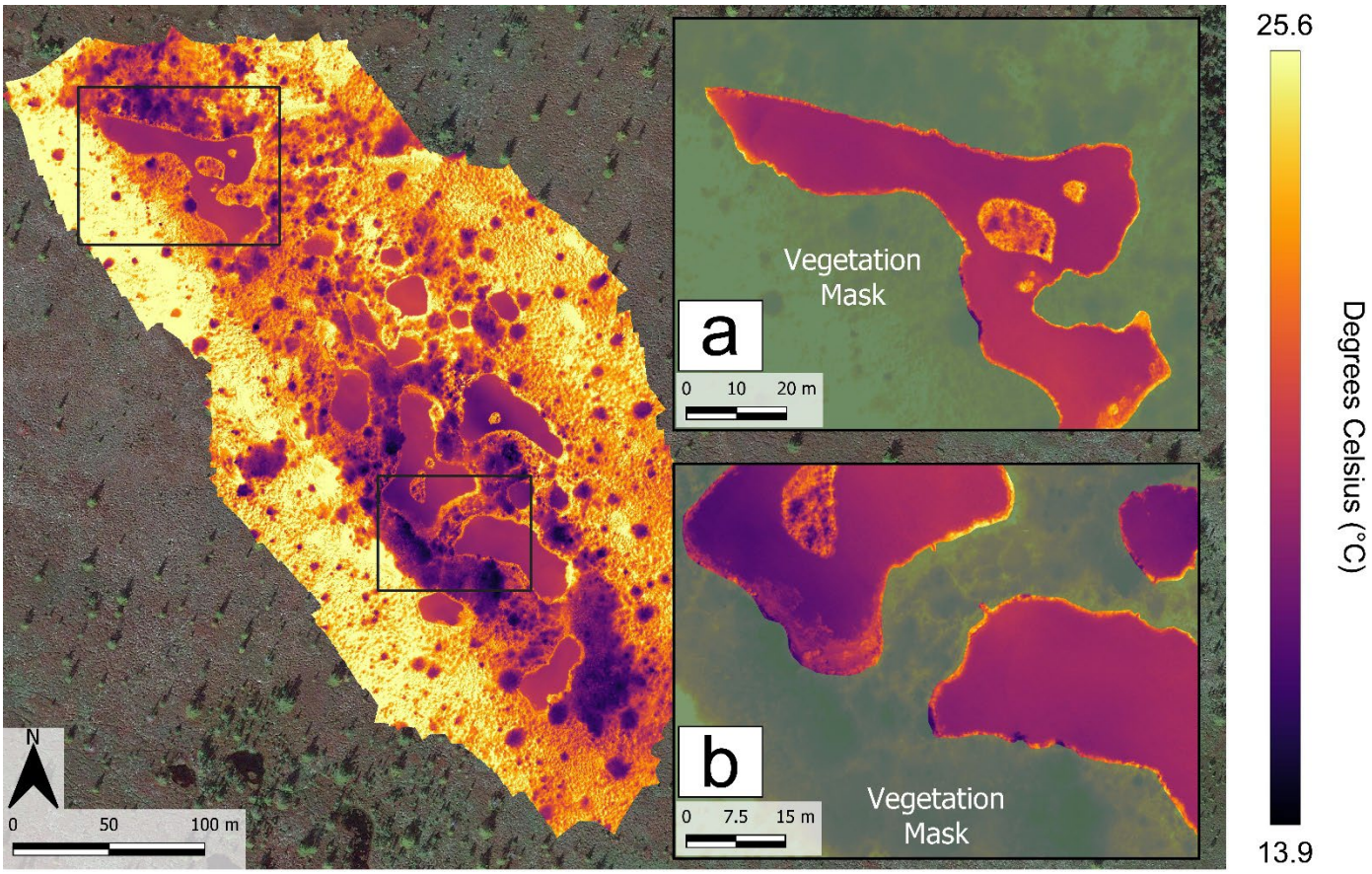

Figure S11: Unmanned Aerial System (UAS) Thermal Infrared (TIR) orthomosaic map, calibrated against the thermal emissivity of water, captured over the patterned pools in Meddybemps Heath on June 15th, 2023. A thermal gradient is not readily observed, highlighted in (a) the northern-most pool and (b) only subtly observed along the western side of the central pools. Resolution of the TIR orthomosaic map is 7.87 cm/pixel. Basemap data: © Microsoft (2024).

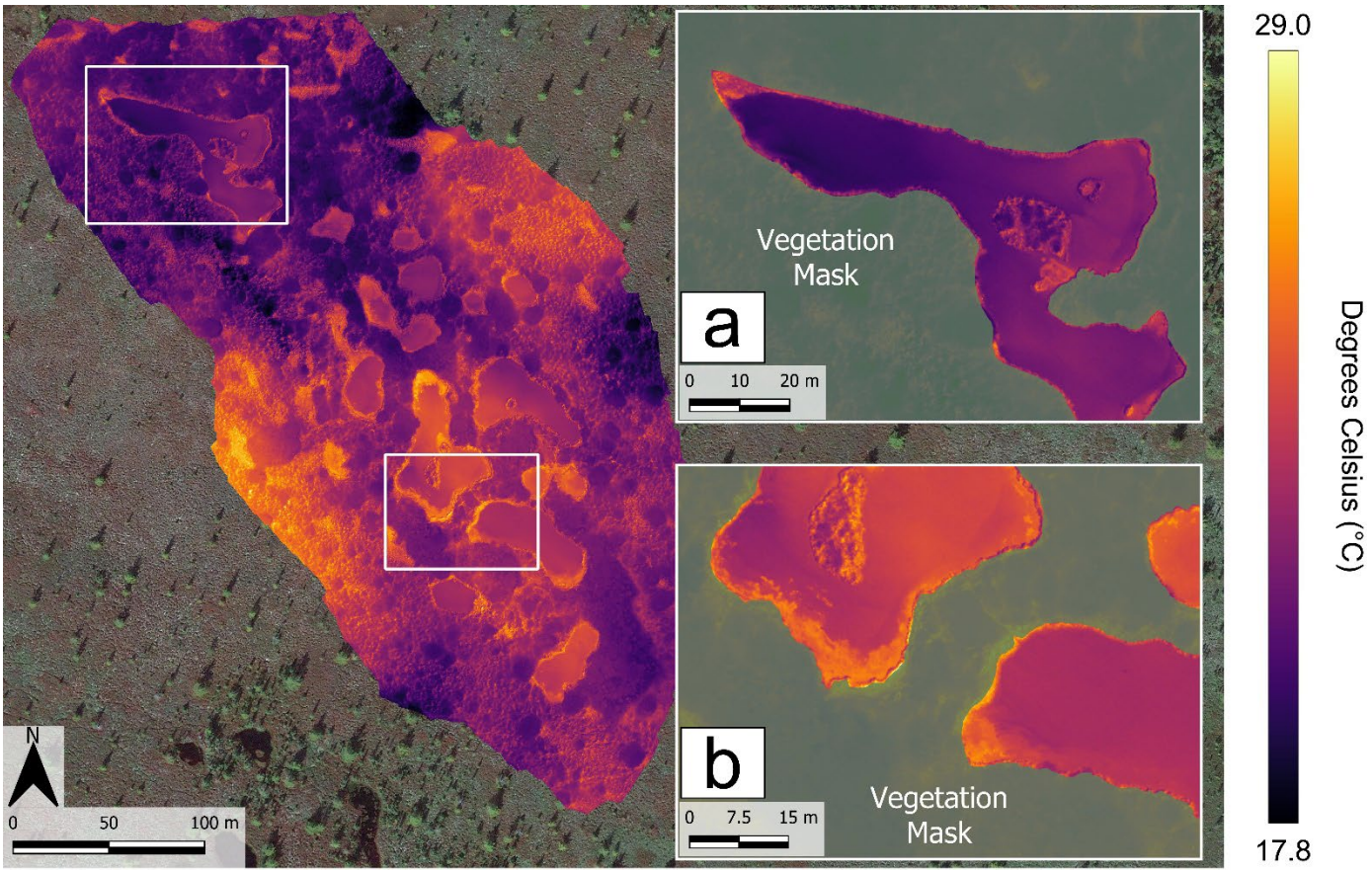

Figure S12: Unmanned Aerial System (UAS) Thermal Infrared (TIR) orthomosaic map, calibrated against the thermal emissivity of water, of the patterned pools in Meddybemps Heath captured on August 9th, 2023. The thermal gradient transitions from cooler to warmer pool water moving eastwards, (a) shows the coolest temperature observed in the pools in the northern-most pool and (b) displays mixing dynamics originating with cooler waters on the western side of the central pools. Resolution of the TIR orthomosaic map is 8.90 cm/pixel. Basemap data: © Microsoft (2024).

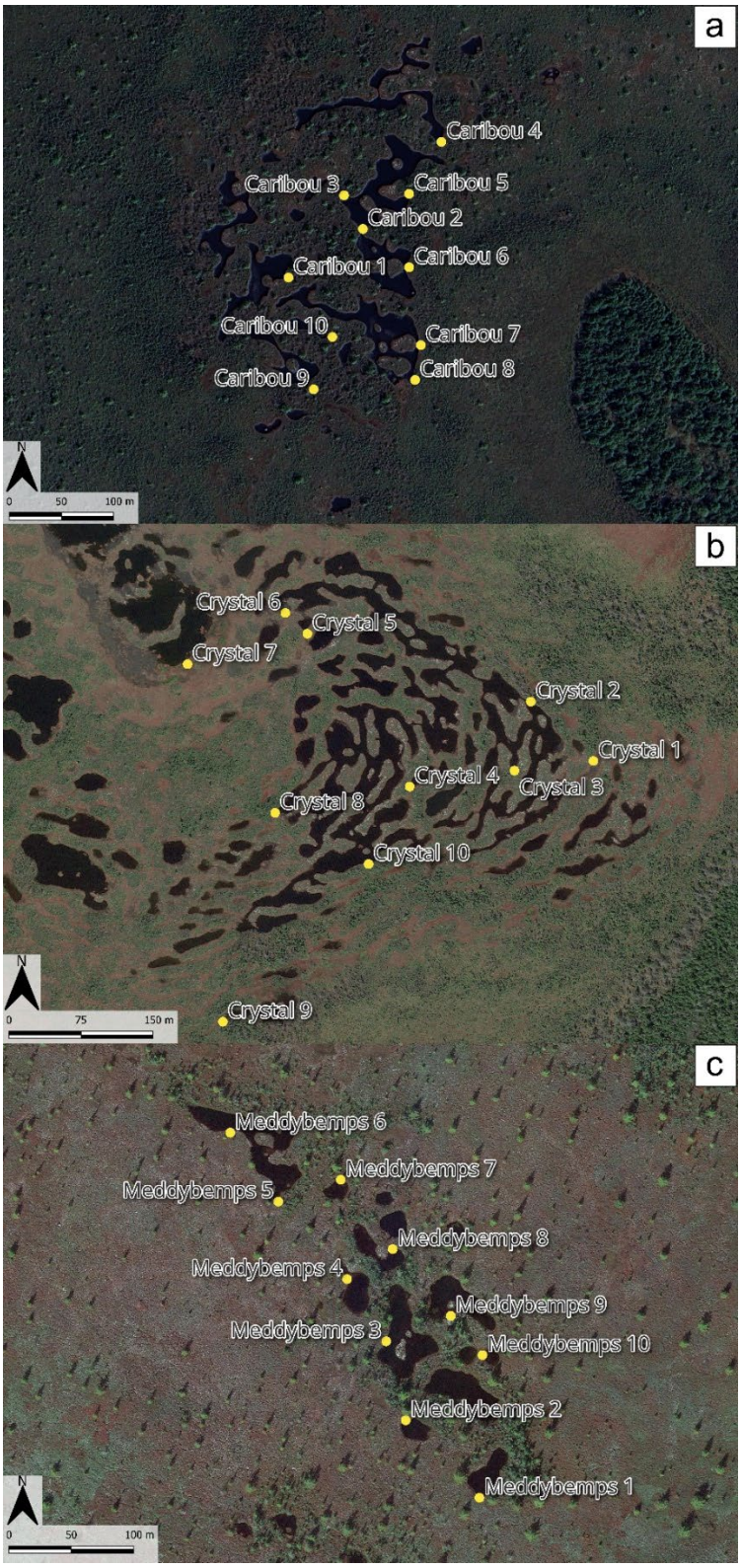

Figure S13: Locations of water samples in a) Caribou Bog, b) Thousand Acre (Crystal) Bog, and c) Meddybemps Heath collected for Inductively-Coupled Plasma Optical Emission Spectrometry (ICP-OES) geochemical analysis of trace elements. Basemap data: © Microsoft (2024).

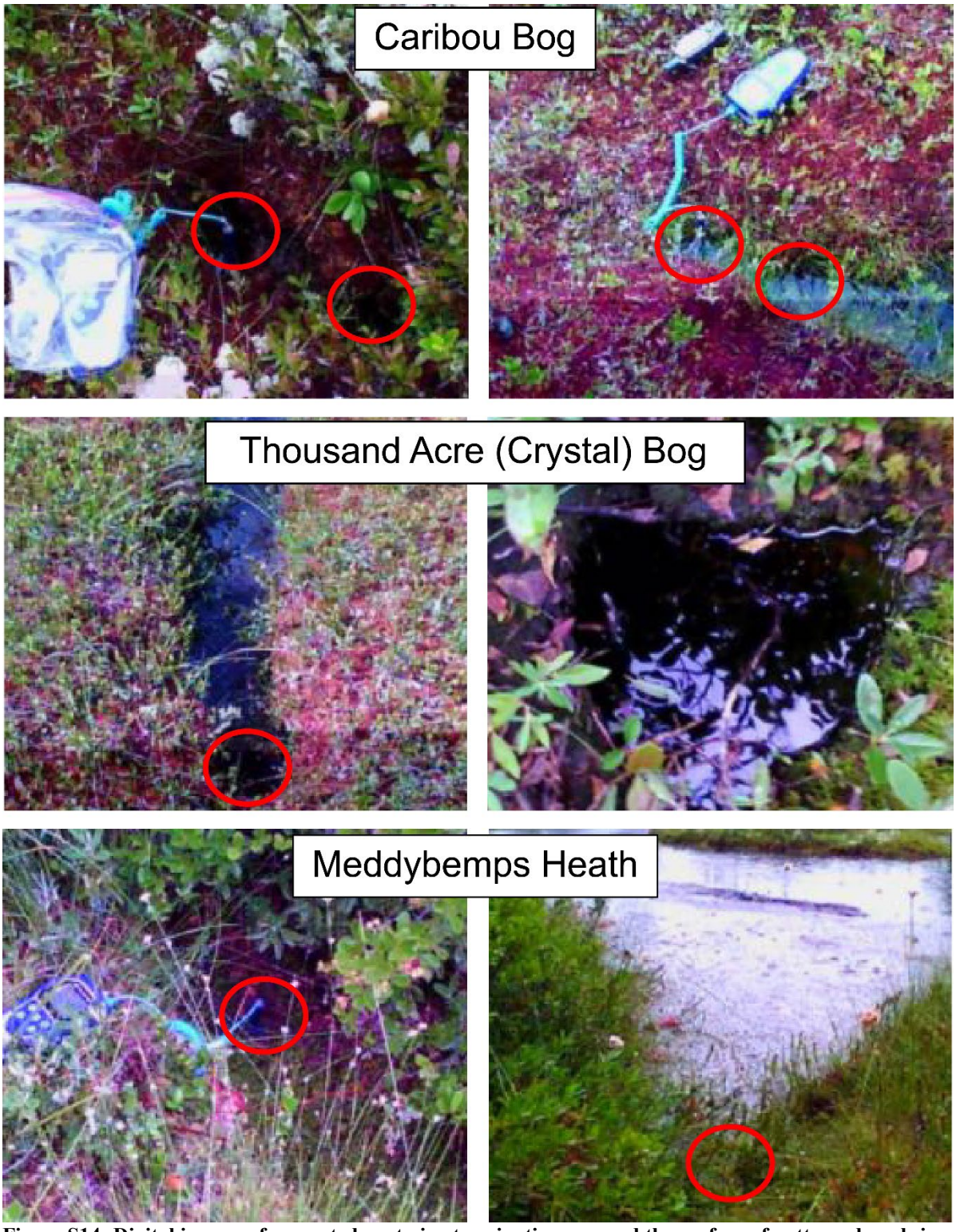

Figure S14: Digital images of suspected peat pipe terminations around the surface of patterned pools in Caribou Bog, Meddybemps Heath, and Thousand Acre (Crystal) Bog. Photographs by Henry Moore, Rutgers University-Newark, 2022-2023.

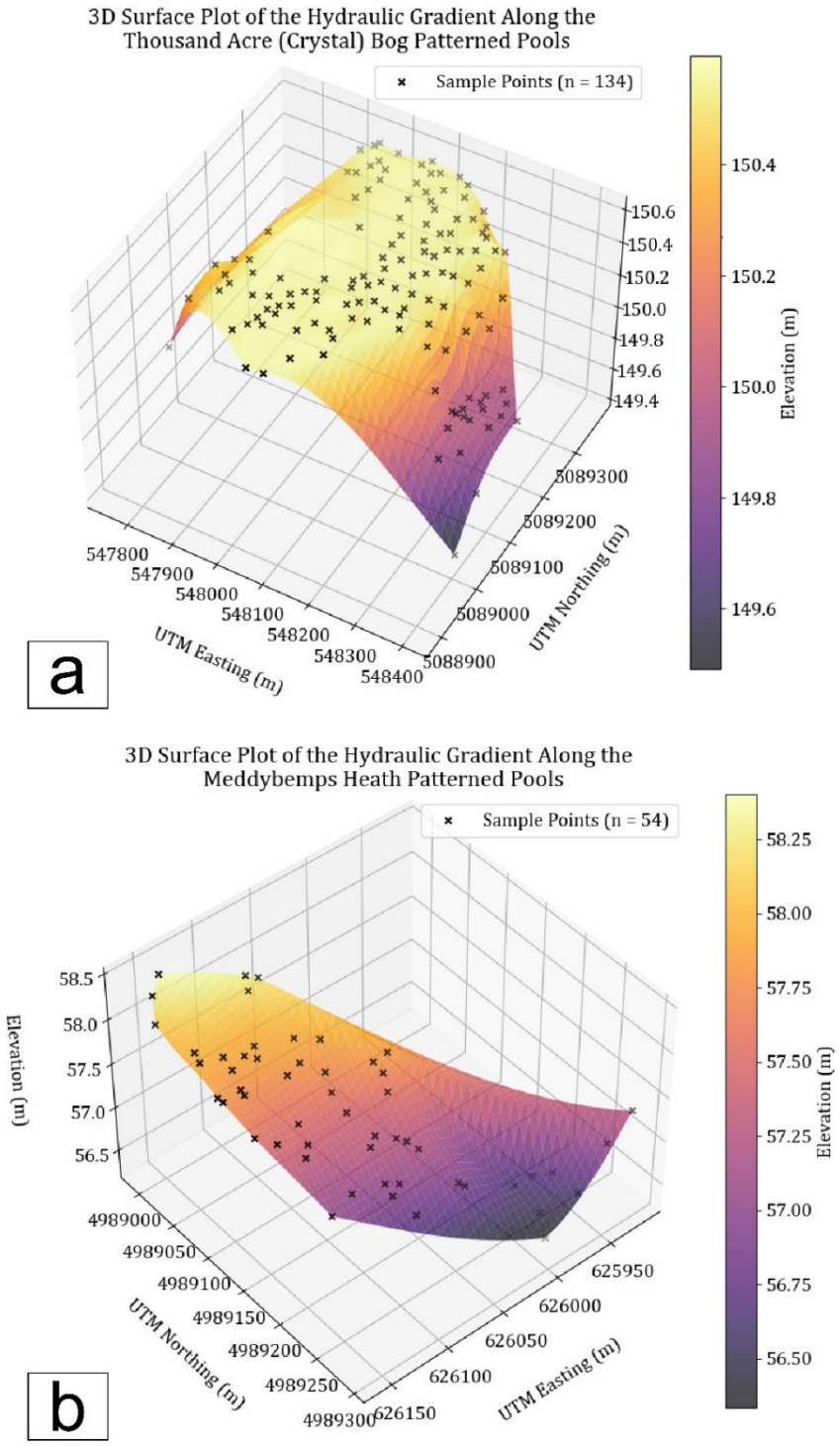

Figure S15: Hydraulic head elevations modeled from points along the patterned pool surface waters in a) Thousand Acre (Crystal) Bog and b) Meddybemps Heath raised northern peat bogs. All elevation data were retrieved from digital elevation maps published by the State of Maine (2020).

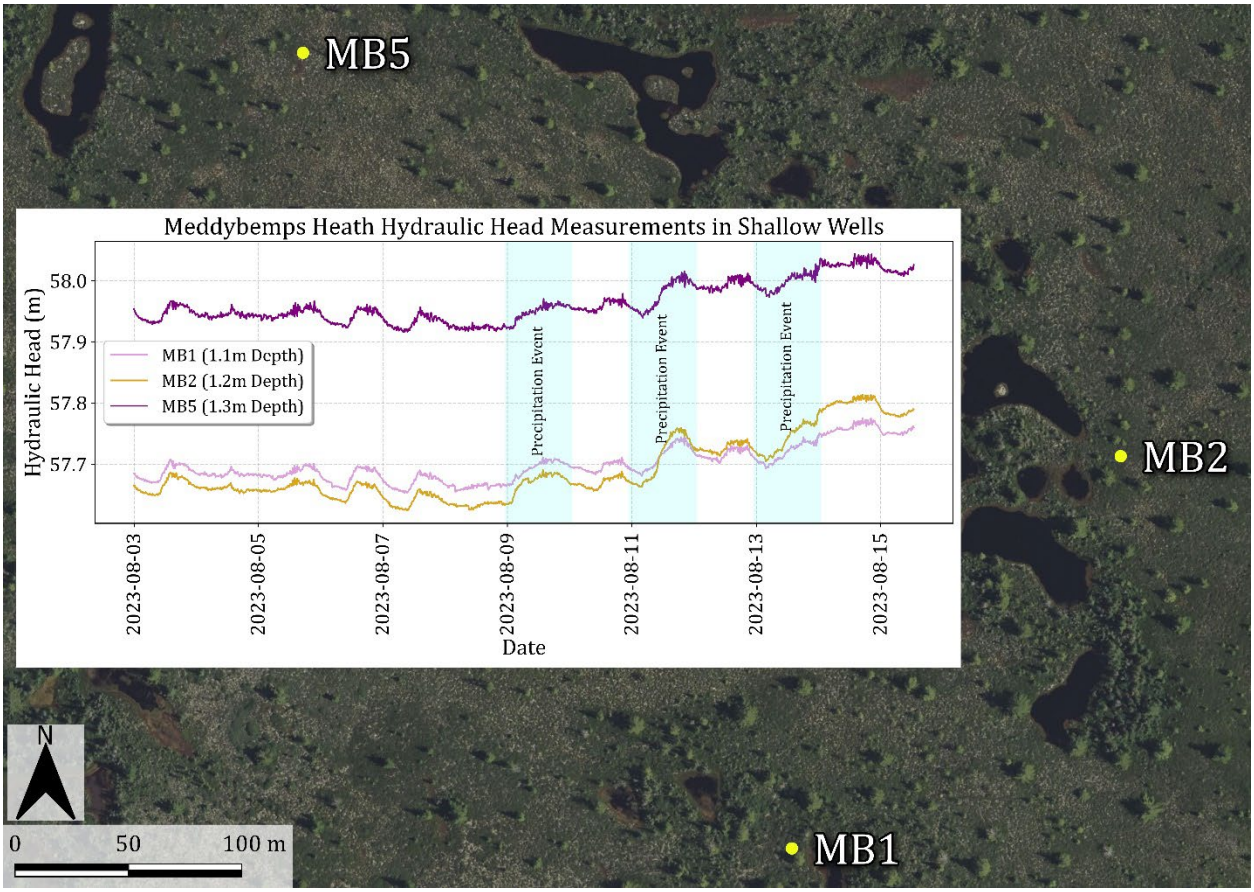

Figure S16: Precipitation responses from the hydraulic head in three shallow wells installed in Meddybemps Heath from August 3rd, 2024, to August 16th, 2024. Basemap data: © Microsoft (2024).

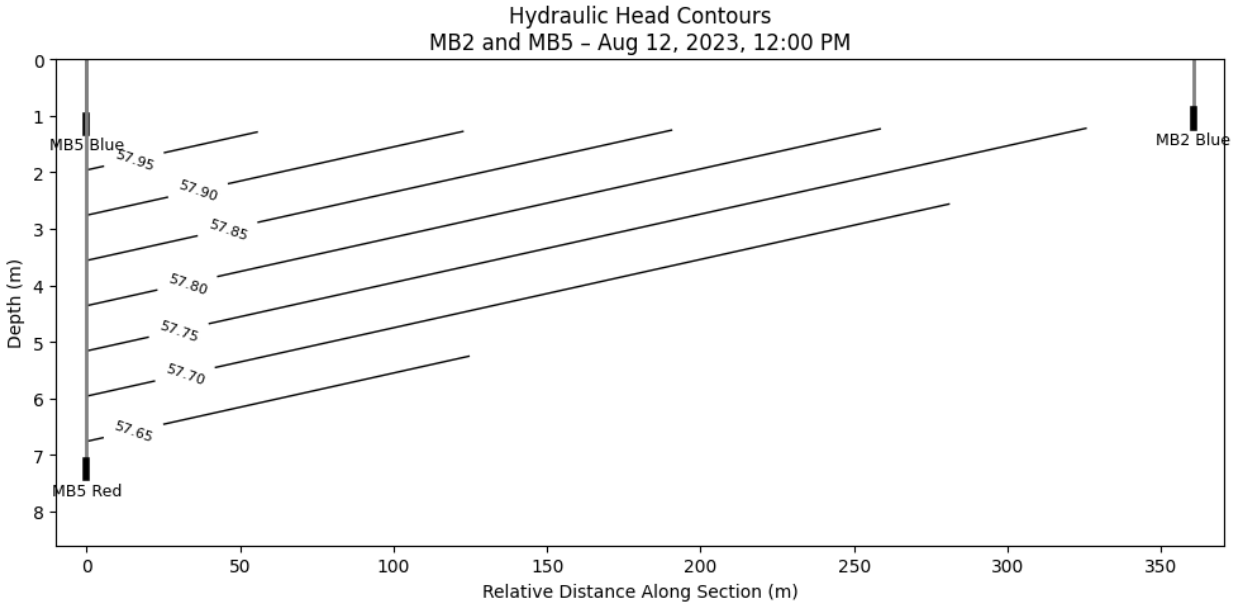

Figure S17: Hydraulic head contours between wells MB5 and MB2 crossing the patterned pools of Meddybemps Heath on August 12th, 2023, showing downwelling between the wells.

Table S5. Agisoft Metashape Professional software (Agisoft LLC, St. Petersburg, Russia) parameters for the June 9th, 2023, Caribou Bog Patterned Pools thermal infrared orthomosaic.

Align Photos (Run Twice)	Surface Type: Arbitrary (3D)
Highest Accuracy	Face Count: High
Generic Preselection	Interpolation: Enabled
Reset Current Preselection	Point Classes: All
Reference Preselection	Calculate Vertex Colors
Estimated	**Build Orthomosaic**
Key Point Limit: 40,000	Type: Geographic
Tie Point Limit: 10,000	WGS84/EPSG 32619
Adaptive Camera Model Fitting	Surface: Mesh
Build Mesh	Blending Mode: Mosaic
Source Data: Tie Points	Enable Hole Filling

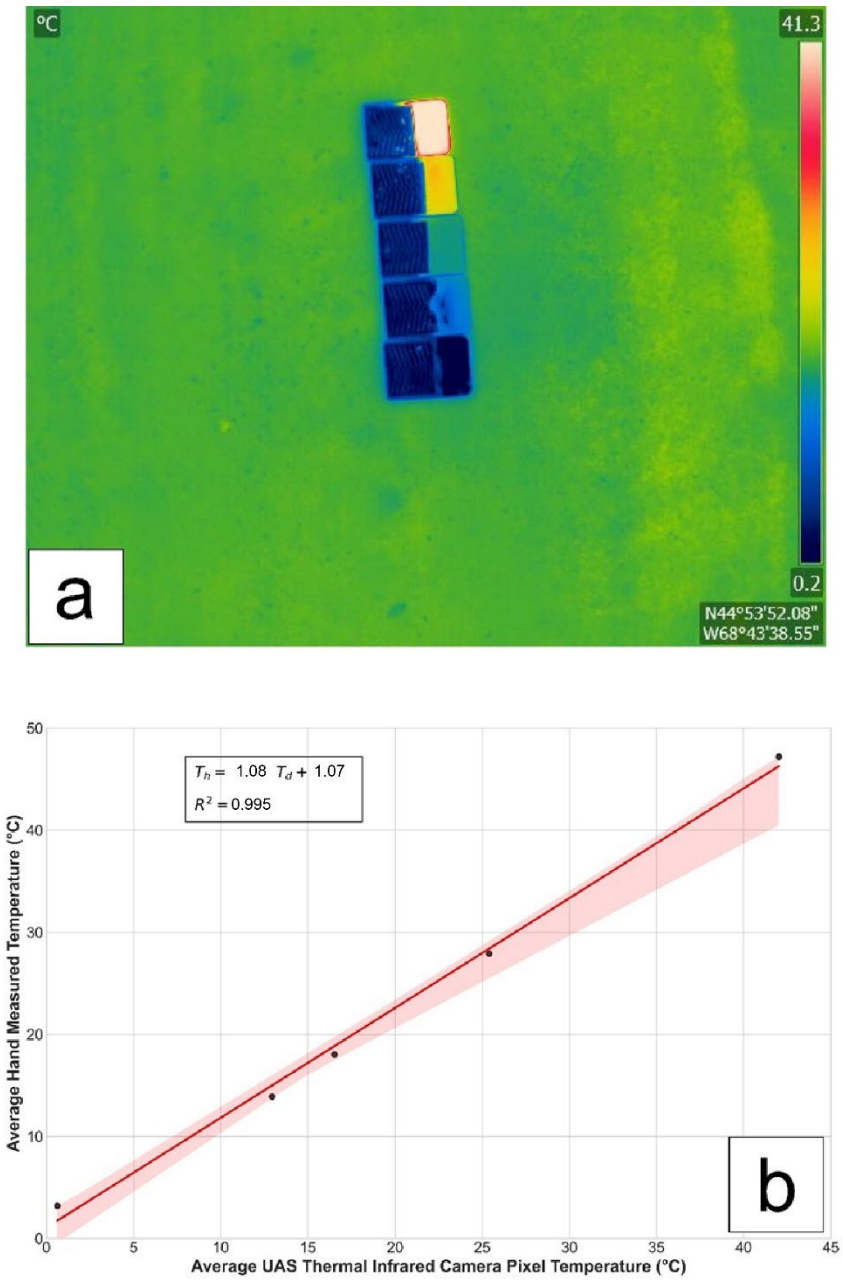

Figure S18: Calibration of thermal infrared (TIR) temperature imagery captured during the June 9th, 2023, Caribou Bog Patterned Pools UAS mission displaying a) TIR calibration image of painting pans with five different temperatures of water sampled for UAS imagery temperature values (T_d) regressed in b) against hand sampled temperature values (T_h) from the pans. The red shaded area represents the regression data area density. Any use of trade, product, or firm names is for descriptive purposes only and does not imply endorsement by the U.S. Government.

Table S6. Agisoft Metashape Professional software (Agisoft LLC, St. Petersburg, Russia) parameters for the November 3rd, 2023, Meddybemps Heath Patterned Pools thermal infrared orthomosaic.

Align Photos (Run Twice)	Surface Type: Arbitrary (3D)
Highest Accuracy	Face Count: High
Generic Preselection	Interpolation: Enabled
Reset Current Preselection	Point Classes: All
Reference Preselection	Calculate Vertex Colors
Estimated	**Build Orthomosaic**
Key Point Limit: 40,000	Type: Geographic
Tie Point Limit: 10,000	WGS84/EPSG 32619
Adaptive Camera Model Fitting	Surface: Mesh
Build Mesh	Blending Mode: Mosaic
Source Data: Tie Points	Enable Hole Filling

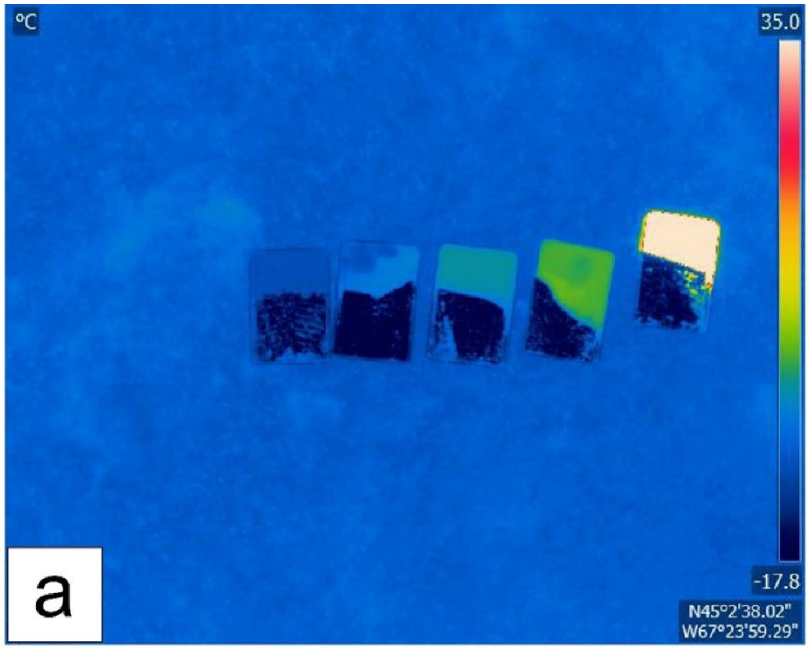

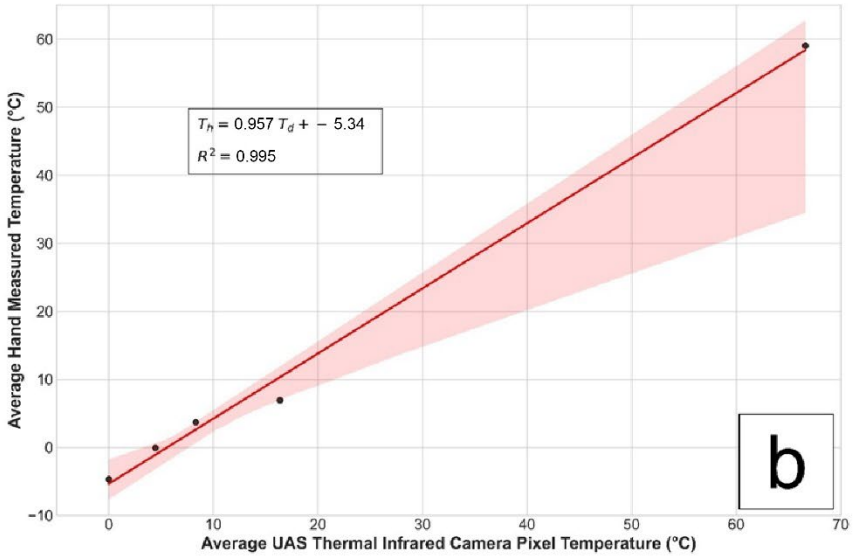

Figure S19: Calibration of thermal infrared (TIR) temperature imagery captured during the November 3rd, 2023, Meddybemps Heath Patterned Pools UAS mission displaying a) TIR calibration image of painting pans with five different temperatures of water sampled for UAS imagery temperature values (T_d) regressed in b) against hand sampled temperature values (T_h) from the pans. The red shaded area represents the regression data area density. Any use of trade, product, or firm names is for descriptive purposes only and does not imply endorsement by the U.S. Government.

Table S7. Agisoft Metashape Professional software (Agisoft LLC, St. Petersburg, Russia) parameters for the August 10th, 2023, Thousand Acre (Crystal) Bog Patterned Pools thermal infrared orthomosaic.

Align Photos (Run Twice)	Surface Type: Arbitrary (3D)
Highest Accuracy	Face Count: High
Generic Preselection	Interpolation: Enabled
Reset Current Preselection	Point Classes: All
Reference Preselection	Calculate Vertex Colors
Estimated	**Build Orthomosaic**
Key Point Limit: 40,000	Type: Geographic
Tie Point Limit: 10,000	WGS84/EPSG 32619
Adaptive Camera Model Fitting	Surface: Mesh
Build Mesh	Blending Mode: Mosaic
Source Data: Tie Points	Enable Hole Filling

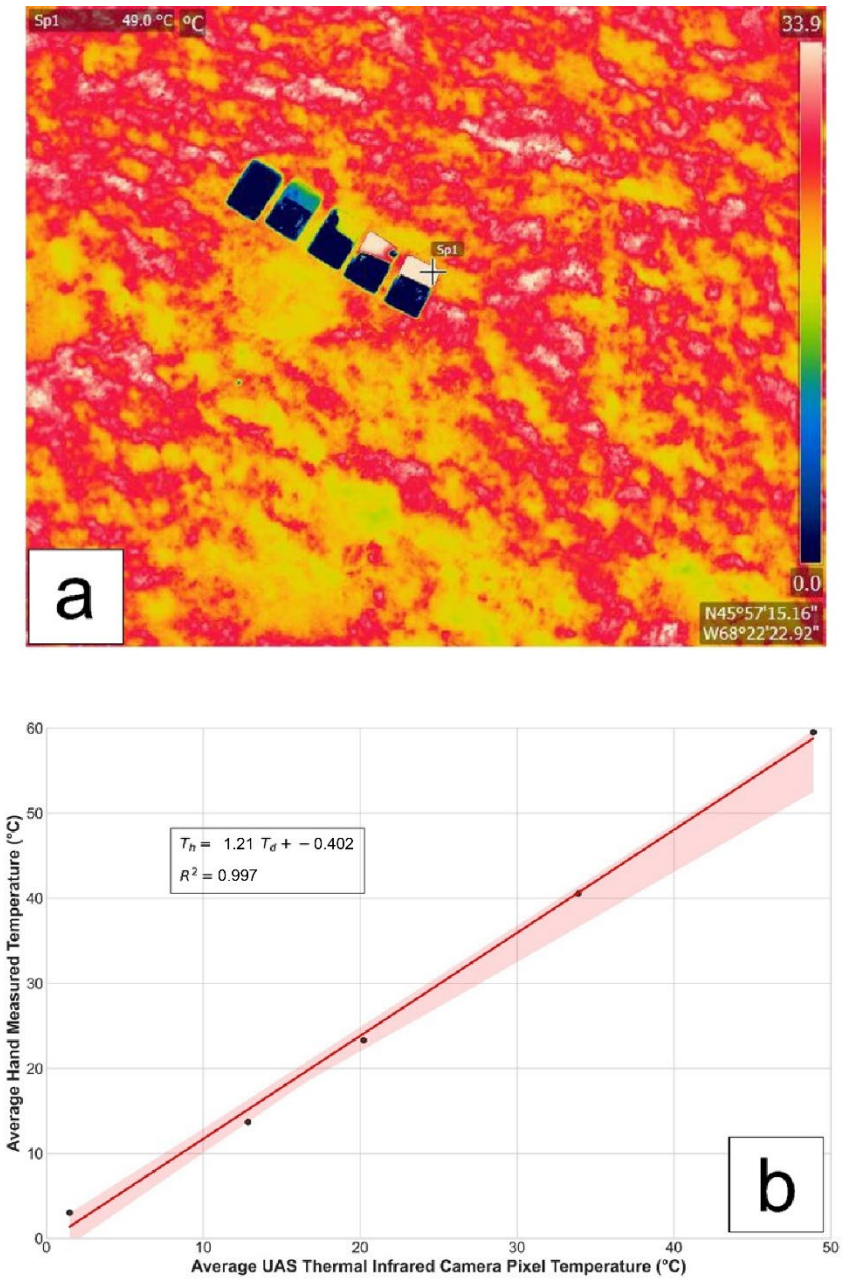

Figure S20: Calibration of thermal infrared (TIR) temperature imagery captured during the August 10th, 2023, Thousand Acre (Crystal) Bog Patterned Pools UAS mission displaying a) TIR calibration image of painting pans with five different temperatures of water sampled for UAS imagery temperature values (T_d) regressed in b) against hand sampled temperature values (T_h) from the pans. The red shaded area represents the regression data area density. Any use of trade, product, or firm names is for descriptive purposes only and does not imply endorsement by the U.S. Government.

Table S8. Agisoft Metashape Professional software (Agisoft LLC, St. Petersburg, Russia) parameters for the June 15th, 2023, Meddybemps Heath Patterned Pools thermal infrared orthomosaic.

Align Photos (Run Twice)	Surface Type: Arbitrary (3D)
Highest Accuracy	Face Count: High
Generic Preselection	Interpolation: Enabled
Reset Current Preselection	Point Classes: All
Reference Preselection	Calculate Vertex Colors
Estimated	**Build Orthomosaic**
Key Point Limit: 40,000	Type: Geographic
Tie Point Limit: 10,000	WGS84/EPSG 32619
Adaptive Camera Model Fitting	Surface: Mesh
Build Mesh	Blending Mode: Mosaic
Source Data: Tie Points	Enable Hole Filling

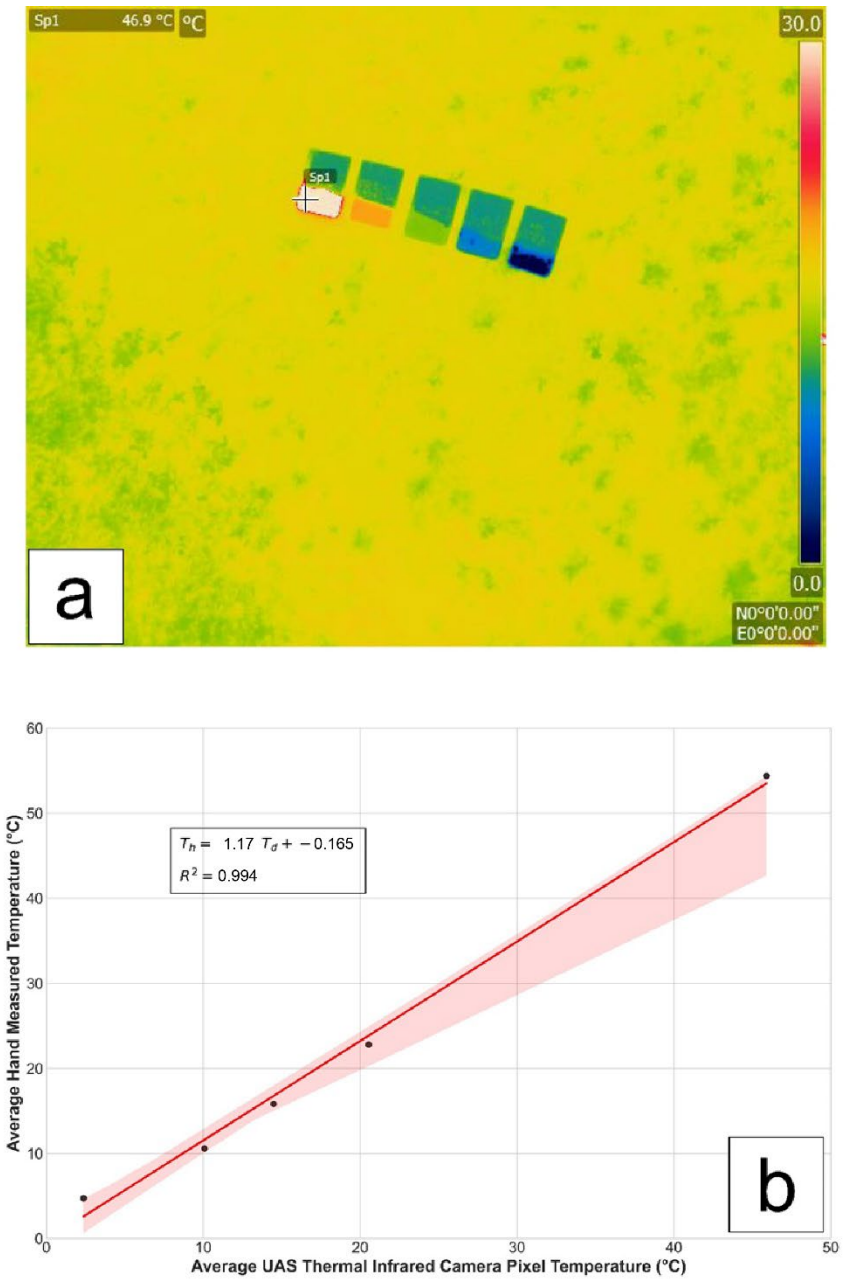

Figure S21: Calibration of thermal infrared (TIR) temperature imagery captured during the June 15th, 2023, Meddybemps Heath Patterned Pools UAS mission displaying a) TIR calibration image of painting pans with five different temperatures of water sampled for UAS imagery temperature values (T_d) regressed in b) against hand sampled temperature values (T_h) from the pans. The red shaded area represents the regression data area density. Any use of trade, product, or firm names is for descriptive purposes only and does not imply endorsement by the U.S. Government.

Table S9. Agisoft Metashape Professional software (Agisoft LLC, St. Petersburg, Russia) parameters for the August 9th, 2023, Meddybemps Heath Patterned Pools thermal infrared orthomosaic.

Align Photos (Run Twice)	Surface Type: Arbitrary (3D)
Highest Accuracy	Face Count: High
Generic Preselection	Interpolation: Enabled
Reset Current Preselection	Point Classes: All
Reference Preselection	Calculate Vertex Colors
Estimated	**Build Orthomosaic**
Key Point Limit: 40,000	Type: Geographic
Tie Point Limit: 10,000	WGS84/EPSG 32619
Adaptive Camera Model Fitting	Surface: Mesh
Build Mesh	Blending Mode: Mosaic
Source Data: Tie Points	Enable Hole Filling

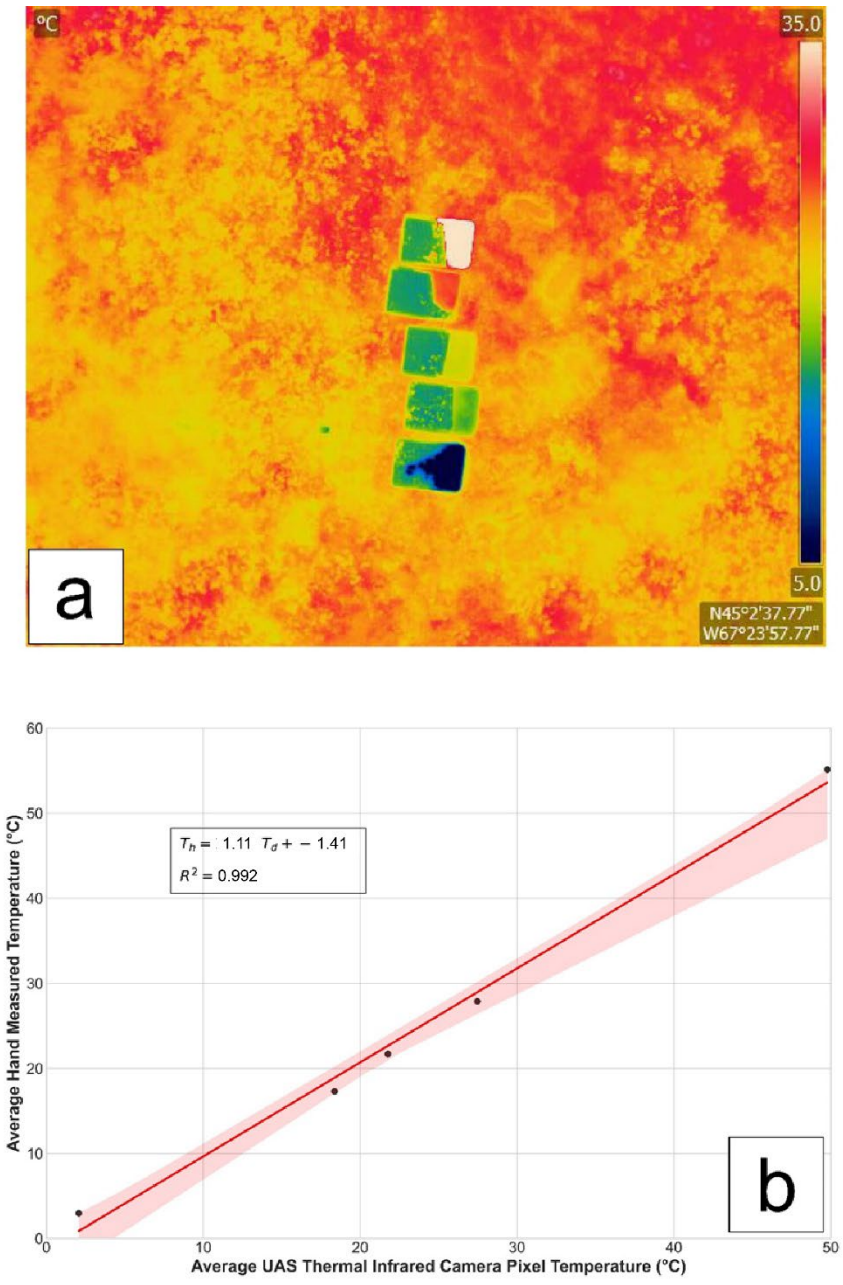

Figure S22: Calibration of thermal infrared (TIR) temperature imagery captured during the August 9th, 2023, Meddybemps Heath Patterned Pools UAS mission displaying a) TIR calibration image of painting pans with five different temperatures of water sampled for UAS imagery temperature values (T_d) regressed in b) against hand sampled temperature values (T_h) from the pans. The red shaded area represents the regression data area density. Any use of trade, product, or firm names is for descriptive purposes only and does not imply endorsement by the U.S. Government.